Environmental Stability of Perovskite

Subjects: Materials Science, Composites

Contributor: Ke Wang

This entry introduces the environmental stability of MAPbI3 perovskite thin film and MAPbBr3 perovskite single crystal.

Keywords: photoemission spectroscopy (PES) ; perovskite thin films ; perovskite single crystals ; environmental stability

1. Background

Since the first application in photovoltaic cells in 2009. Organic−inorganic halide perovskites have received considerable attention and have been the focus of the enormous research effort in the past few years due to their outstanding performance in optoelectronic devices. The power conversion efficiency (PCE) of the perovskite solar cells (PSCs) raised from 3.8% in 2009 to 25.5% in 2020 only for a decade of development, given their superb properties such as long diffusion length, long carrier lifetime, tunable bandgap and high absorption coefficient. In addition, ease of fabrication and low production cost make them competitive to the traditional silicon-based solar cells. With these unique features, PSCs are a suitable choice for the next generation of photovoltaic devices. Although the performance of the PSCs has been heavily investigated, the long-term stability is still the biggest concern in the research community that prevents them from further commercial applications.

There are a lot of factors that limit the stability and performance of perovskites, like moisture, oxygen, light irradiation, which have been found and investigated by the research community. Niu *et al*. found that $CH_3NH_3PbI_3$ ($MAPbI_3$) could degrade in the presence of moisture and Al_2O_3 could successfully protect the perovskite layer [1]. Aristidou *et al*. reported that $MAPbI_3$ photoactive layers rapidly decompose into CH_3NH_2, PbI_2, and I_2 after oxygen and light exposure, which is triggered by the reaction of superoxide (O_2^-) with the $CH_3NH_3^+$ cation from the perovskite absorber [2]. Philippe *et al*. studied performance of both $MAPbI_{3-x}Cl_x$ and $MAPbI_3$ under higher temperatures. The perovskite films were heated in an ultra-high vacuum (UHV) chamber without the presence of air and moisture and degraded when the temperature approached 100 °C [3]. Lee *et al*. observed UV degradation on PSCs after a 1000-h exposure of 365 nm UV light under inert gas at <0.5 ppm humidity without encapsulation [4]. Nie *et al*. showed their PSCs formed light-activated meta-stable trap states under constant light illumination, which is caused by photocurrent degradation [5]. In addition to the MA-based perovskite, Formamidinium (FA) based perovskites have been reported more stable than pure MA-based perovskites under high temperature, as the molar mass of FA is larger than MA. [6][7] There are also investigations on other factors, such as Iodine vapor, voltage, device structure and mechanical stress [8][9][10][11][12].

2. Environmental Stability of Perovskite Thin Films

2.1. $MAPbI_3$ Thin Film Stability with Air Exposure

Figure 1 shows the X-ray photoemission spectroscopy (XPS) spectrum that before and after the exposure [13]. Only C, N, I and Pb peaks can be observed and no other elemental features can be found in Figure 1a. The elemental ratio of C:N:Pb:I:O is 1.29:1.07:1.00:2.94:0 which was similar to the ideal stoichiometry of $MAPbI_3$ and better to those from spin-coated ones. For the perovskite thin film after air exposure, the red marks show the appearance of gold and oxygen peaks, and the blue mark stands for the disappearance of the N 1s peak. Therefore, the ratio changed to C:N:Pb:I:O = 2.22:0:1.00:1.26:0.58. This can be attributed to the absorption of moisture from the environment, thus caused the film to degrade into PbI_2. It has also been reported that $MAPbI_3$ film became less n-type after a 15-min exposure to ambient air [14].

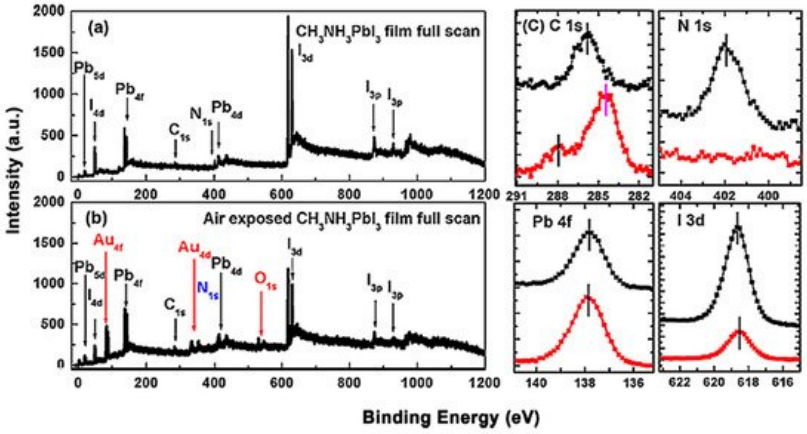

Figure 1. (**a**) XPS full scan of co-evaporated $MAPbI_3$ thin film and (**b**) XPS full scan of air-exposed film. (**c**) XPS spectra comparisons of C 1s, N 1s, Pb 4f, and I 3d core levels. From Ref. [15] with permission.

However, the effects of air exposure are controversial since some reports show that moderate exposure to ambient air could improve crystallinity, grain size, carrier mobility, and charge carrier lifetime of perovskites, thus leading to a better performance of PSCs [16][17][18]. This is contrasted with our observation and the claim that moisture in the air can accelerate the degradation of perovskites [19][20].

2.2. $MAPbI_3$ Thin Film Stability with Oxygen Exposure

Oxygen, as the second-largest composition of air, is considered a potential trigger of perovskite degradation. There are several studies showed that moisture and oxygen could affect the performance of PSCs severely. Sun *et al*. observed that oxygen-induced degradation is triggered at the surfaces and grain boundaries, which is irreversible and can occur at oxygen levels as low as 1% under light illumination [21]. However, most reports focused on the effects of oxygen and moisture together, while this work discusses the effects from each factor independently.

XPS core level spectra of the $MAPbI_3$ film under O_2 exposure and dry air exposure are shown in Figure 2 [22]. Langmuir (L, 1 L = 10^{-6} Torr·s) is used to measure gas adsorption in a UHV system as a unit of exposure to a surface. No obvious change was observed during the exposure in terms of peak positions and intensities. No oxygen signal can be found even after 10^{13} L of exposure. There is also no apparent change in the binding energies (BEs) of C 1s, I 3d, and Pb 4f [22]. From these spectra, it can be seen that there is no change of the film composition and structure without the presence of moisture. These results indicate that the evaporated film is inert to oxygen. Similarly, Kim *et al*. also confirmed that minimal oxygen exposure does not damage the final perovskite structure [24].

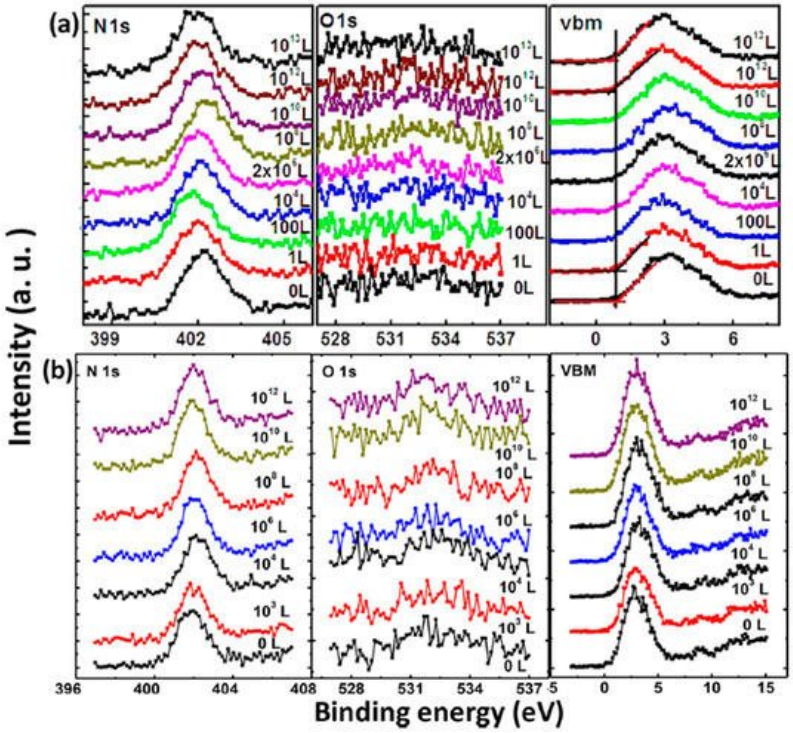

Figure 2. XPS spectra of N 1s, O 1s, and the VBM region of co-evaporated $MAPbI_3$ thin film during (**a**) oxygen exposure and (**b**) dry air exposure From Ref. [25] with permission.

2.3. $MAPbI_3$ Thin Film Stability with Water Exposure

Based on the observations above, we learned that water is the most concerned environmental factor that initiates the degradation process of perovskites. Air exposure was conducted at RT and RH of 41%. The spectra were normalized to the same height in order to be compared properly except for those of N 1s because the signal vanished as the exposure proceed. Both structural and compositional trends of the two measurements are similar. There is no significant change of the spectral shape for perovskite carbon peak C 1s-A and nitrogen peak N 1s before 60 min of air exposure and 1×10^{10} L of water exposure (Stage one). O 1s peak intensity was not increasing in this stage either. In Figure 3b, after 1×10^{10} L of water exposure, Fermi level moved from 0.85 to 1.41 eV in the VBM region and almost reached the bottom of the conduction band (CB) as the bandgap of $MAPbI_3$ is 1.55 eV [22]. This indicates that water heavily n-doped perovskite in this stage, while the integrity of the sample remains unchanged. This has been related to the metallic Pb surface defects and the position of E_F in the bandgap sensitively shifts with the density of these surface states [26][27].

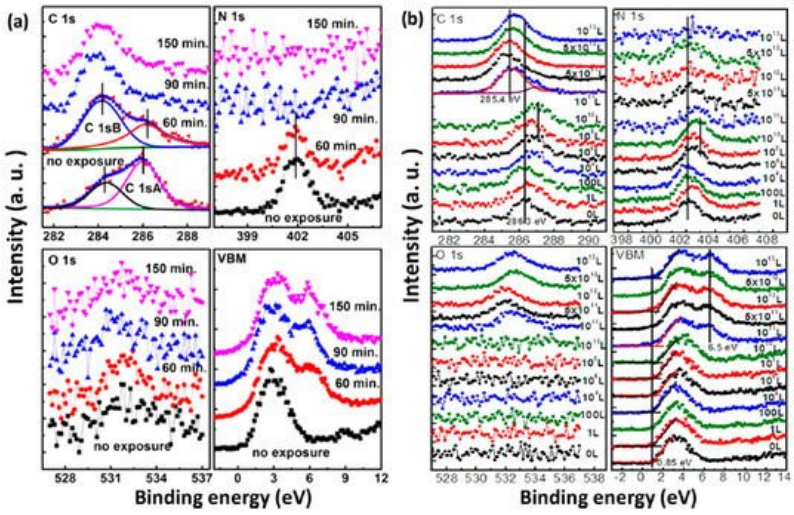

Figure 3. XPS spectral evolutions of C 1s, N 1s, O 1s, and the VBM region of evaporated $MAPbI_3$ thin film during (**a**) atmospheric air exposure and (**b**) H_2O exposure. From Ref. [25] with permission.

The sample was observed to have dramatic change after 60 min of air exposure and 1×10^{10} L of water exposure (Stage two). In the air exposure, the intensity of perovskite carbon peak C 1s-A started to decrease, while amorphous carbon peak C 1s-B and leftover carbon from the degradation of perovskite began to increase. In water exposure, C 1s peak shifted from 286.3 eV (MA^+) to 285.4 eV, which represents the decomposition of MA^+ into hydrocarbon complex. After 90 min and 5×10^{11} L of exposure of air and water, the carbon from perovskite was almost disappeared. Similarly, N 1s signal was gone after 150 min and 10^{12} L of exposure to air and water, respectively, while the O 1s peak from water adsorption appeared and developed significantly. There is almost no change in the intensity of Pb 4f, while the I/Pb ratio dropped to 2.1 when the exposure ended. These show that water in the air triggers the decomposition of perovskite.
Based on the discussion above, the degradation mechanism of the evaporated $MAPbI_3$ thin film under air exposure was expressed as

$$CH_3NH_3PbI_3 \overset{H_2O}{\rightarrow} (-CH_2-) + PbI_2 + NH_3 \uparrow + HI \uparrow$$

The reaction between $MAPbI_3$ and H_2O results in a hydrocarbon complex (most likely polyethylene-like (−CH2−CH2−)) [30]. PbI2, and absorbed water. Nitrogen and part of Iodine left the surface as gases. This agrees well with water catalytic model proposed by other groups [1][31]. The degradation process is irreversible as the gaseous species leave the sample surface. However, it has been reported that perovskite monohydrate phase was identified with in-situ grazing-incidence X-ray diffraction (GIXRD) after ~170 min exposure to RH over 80%, which could be attributed to water physisorption [29].

2.4. $MAPbI_3$ Thin Film Stability with Light Exposure

Besides the environmental factors discussed above, light illumination is also another potential trigger of decomposing the perovskite and a number of researchers have been studying this issue. Leijtens *et al*. claimed that the light-induced degradation of PSCs can be attributed to the TiO_2 layer in the device [8]. Murugadoss *et al*. revealed a strong substrate dependence of perovskite thin films [33]. Bryant *et al*. studied perovskite stability in gases and ambient environment and found that light illumination was the main factor causing the degradation [34]. Das *et al*. also reported that the chemical

properties of their spin-coated $MAPbI_3$ film change upon illumination in vacuum with the formation of metallic Pb and then by conversion into PbI_2. These changes can be restricted by applying an extraction voltage to the device contacts which leads to the extraction of the photogenerated charges from the absorber [35]. Zhao *et al*. found that $MAPbI_3$ thin films are strained which is caused by the mismatched thermal expansion during the annealing process, thus increases ion migration in strained perovskites films and accelerates degradation of perovskite films under light illumination [36]. Yuan *et al*. showed that ion migration caused by electric current can accelerate the decomposition of $MAPbI_3$ [37]

The photostability investigation of the $MAPbI_3$ thin film with XPS is shown in Figure 4. The laser has a wavelength of 408 nm and the intensity is ~7 times the AM 1.5 irradiation [38]. For the laser irradiated spot, all peaks began to shift to the higher BE region after 120 min of light exposure and saturated after 480 min. A new Pb component showed up at 136.87 eV after 120 min of illumination, which is synchronized with the new feature in the VBM region at 6.5 eV. This new Pb peak represents a new chemical component and was caused metallic Pb to form, which has previously been reported at 137.0 eV for the Pb $4f_{7/2}$ and was synchronized with the new peak at 6.5 eV in the VBM region [39][40]. The intensity of the N 1s and I 3d were also reduced during irradiation. With these observations, it is clear that the film was first decomposed into PbI_2 by light irradiation and was further degraded into metallic Pb and iodine. Therefore, excess Pb may cause the sample became n-doping, which is similar to the high temperature annealing of perovskite [41]. The metallic Pb can heavily limit the performance of the device by acting as a quenching center of excitons. For the nonirradiated spot, there is no obvious change for all the peaks.

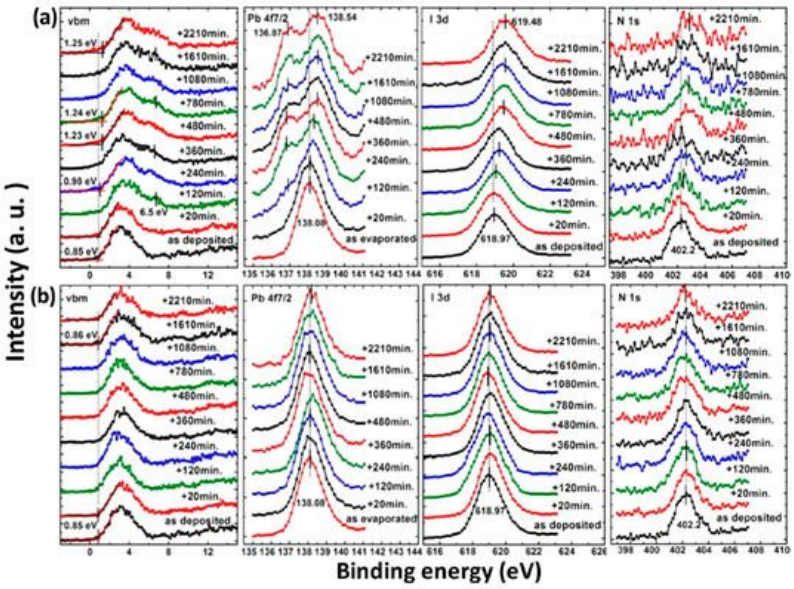

Figure 4. XPS spectra of co-evaporated $MAPbI_3$ thin film at (**a**) laser irradiated and (**b**) nonirradiated positions. From Ref. [42] with permission.

The light-induced degradation process discussed above can be expressed as the two following steps [38]

$$CH_3NH_3PbI_3 \overset{Light}{\rightarrow} (-CH_2-) + PbI_2 + NH_3 \uparrow + HI \uparrow$$

$$PbI_2 \overset{Light}{\rightarrow} Pb + I_2 \uparrow$$

The volatile species, NH_3 and HI leave the surface in the first step, and so does the iodine in the second step by sublimation, leaving the remaining $MAPbI_3$, metallic Pb, and hydrocarbon complex components on the surface. This is also observed by other groups [2][43]. In contrast, Das *et al*. suggested that photodegradation of $MAPbI_3$ film occurs in two steps in vacuum. First, iodine vacancies were created by vacuum in perovskite, then light-induced charge carriers react with perovskite, forming organic dissociates. These iodine vacancies can trap the photogenerated electrons before the recombination, then Pb^{2+} could acquire the electron and convert to metallic Pb [35][44]. The vacuum could also accelerate

the removal of the volatile species from the perovskite. However, in various literature, it has been reported that the metallic Pb can convert back to perovskite when rest in the dark and cation migration in the dark can enhance the decreased performance of the PSCs [5][45].

3. Environmental Stability of Perovskite Single Crystals

3.1. $MAPbBr_3$ Single Crystal Stability with X-ray Exposure

In Figure 5a, a second Pb component (Pb-B) started to show up at ~136.04 eV from the second scan as marked by the red arrow, which is identified as the metallic Pb, while the perovskite Pb-A peak is at ~138.05 eV. As shown in Figure 6, the core level of all elements has no significant change, except for Pb.

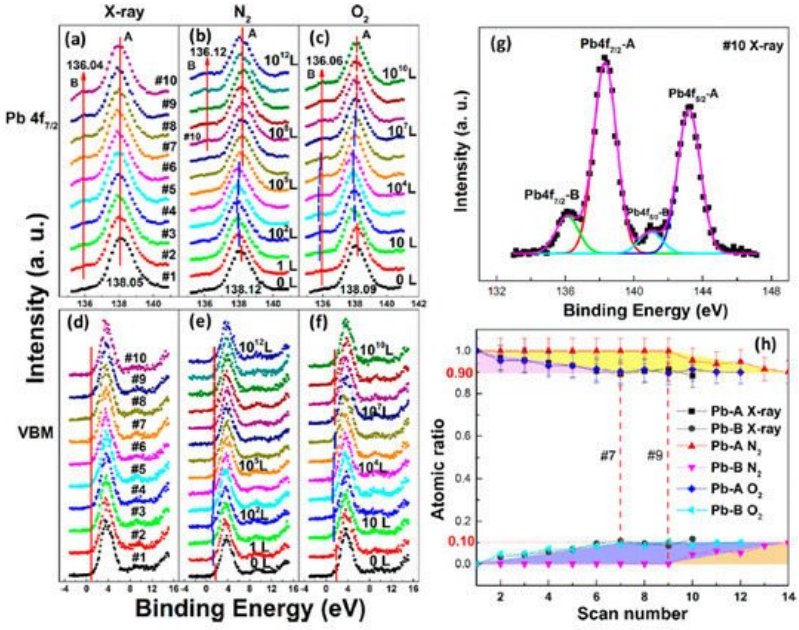

Figure 5. (**a**–**f**) XPS spectral evolutions of Pb $4f_{7/2}$ and VBM of cleaved $MAPbBr_3$ single crystal under X-ray, N_2, and O_2 exposures, respectively. (**g**) The detailed fitting curves for Pb under the 10th X-ray scan. (**h**) Elemental ratio comparisons of Pb peaks under the three conditions with error bars. From Ref. [46] with permission.

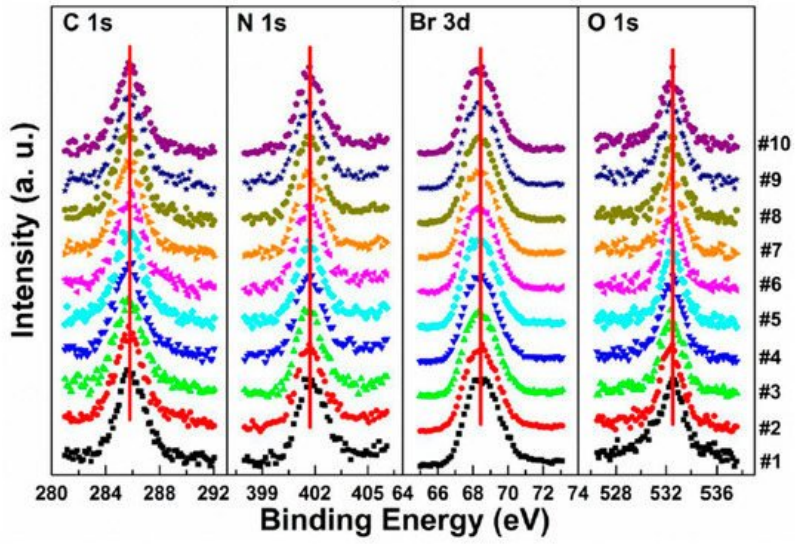

Figure 6. Evolutions of C 1s, N 1s, Br 3d, and O 1s XPS spectra of cleaved $MAPbBr_3$ single crystal under X-ray exposure. From Ref. [46] with permission.

A possible reaction is proposed to explain the conversion of metallic Pb under X-ray exposure [47].

$$CH_3NH_3PbBr_3 \overset{X-ray}{\rightarrow} CH_3NH_3Br + Pb + Br_2 \uparrow$$

By comparing the elemental ratios of the whole process, 10% Pb-A converted to Pb-B, which suggests that 10% of the perovskite decomposed after 10-h X-ray exposure. C 1s peak position is ~285.81 eV and no amorphous carbon showed up at ~284.6 eV at either the test spot (Figure 6) or the control spot (Figure S1 (see supplementary materials)). It shows that the increased carbon was not from the contamination in the UHV chamber, which may suggest that it could be attributed to the surface diffusion of MABr.

3.2. $MAPbBr_3$ Single Crystal Stability with Nitrogen Exposure

Although N_2 is normally used to protect the sample as an inert gas during the perovskite environmental studies [20][48][49][50]. the role of N_2 in the degradation process remains to be clarified.

Figure 5b,e and Figure 7 are associated with N_2 exposure. Before 10^7 L, it can be observed that all peaks and VBM started to move toward the low BE direction and reach the maximum at 10^2 L by about 0.31 eV, then shifted back to the original position at 10^5 L. This represents that the perovskite crystal was slightly p-doped by nitrogen via physical absorption and N_2 slowly left the surface afterward. There is no metallic Pb nor other elemental ratio change at 10^7 L with 9-h X-ray exposure, suggesting that the sample surface can be protected from X-ray degradation with N_2 for up to 9 h and stop MABr diffusion at the same time. However, metallic Pb peak started to show up at 10^8 L and increased to 10% of the total Pb at 10^{12} L (14-h XPS scan). The degradation process is the same as discussed in Equation (5). It can be concluded that N_2 could protect perovskite crystal from XPS X-ray degradation for 9 h as it p-doped perovskite by ~0.31 eV first then slowly left the surface.

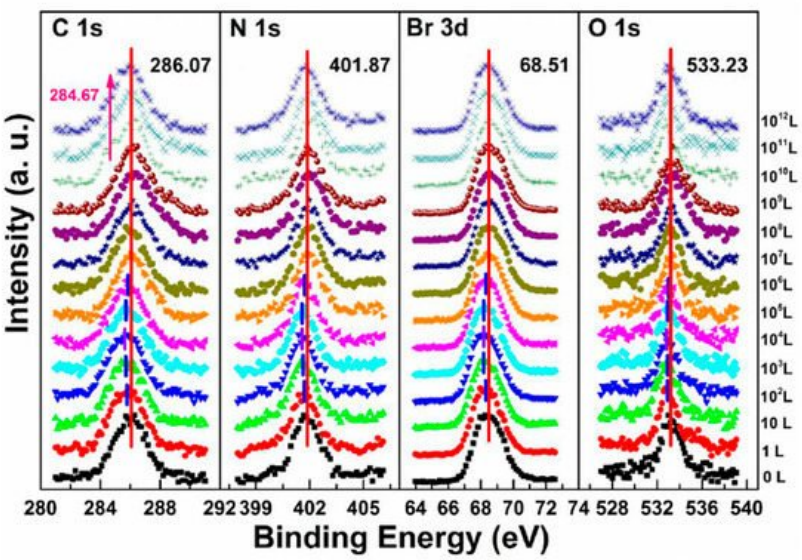

Figure 7. Evolutions of C 1s, N 1s, Br 3d, and O 1s XPS spectra of cleaved $MAPbBr_3$ single crystal under N_2 exposures. From Ref. [46] with permission.

3.3. $MAPbBr_3$ Single Crystal Stability with Oxygen Exposure

In the previous discussion of perovskite thin films, O_2 does not react with the sample and only acts as a p-dopant during the exposure. It's also important to know if it acts the same with perovskite SCs.

The metallic Pb peak began to develop from the second scan as under the X-ray exposure, which suggests that O_2 cannot shield the sample as N_2 did under the same condition, as shown in Figure 5c,f. The peak position and the ratio changes indicate that the exposure process consists two steps. In step one, all peaks started to move to the lower BE direction from 1 L and reached the maximum at 10^4 L, except O 1s. The VBM also had the same pattern with a maximum shift of ~0.18 eV, which is the same as the oxygen exposure on perovskite thin films [22]. Meanwhile, O 1s started to move to the higher BE region from the beginning and achieved the maximum of ~534.09 eV at 10^4 L. These firmly suggested that the detected O 1s mostly came from the crystal surface by O_2 p-doping.

Figure 8 shows that a second carbon peak at ~287.71 eV (C 1s-B) and a second oxygen peak at ~532.56 eV (O 1s-B) appeared after 10^4 L in step two, which indicates the doped oxygen started to bond with carbon and formed C−O bond, at 10^{10} L. Similar to perovskite thin film, perovskite SC also does not react with O_2.

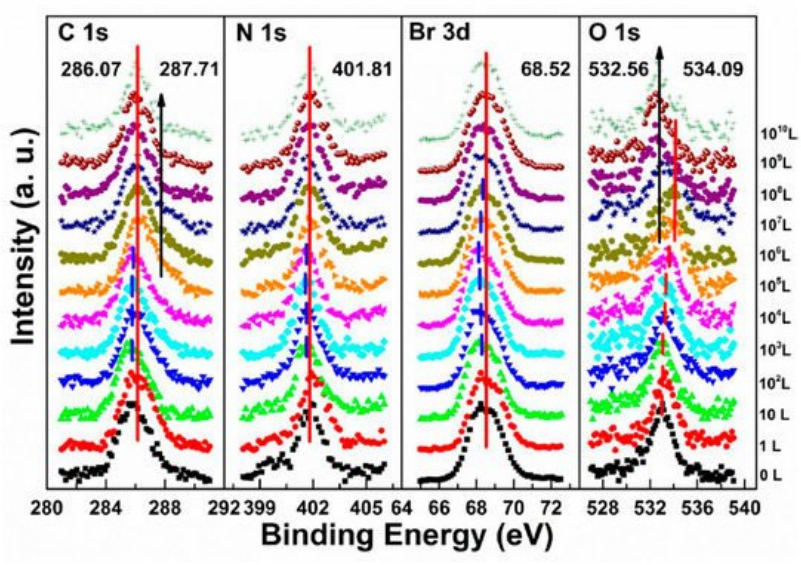

Figure 8. Evolutions of C 1s, N 1s, Br 3d, and O 1s XPS spectra of cleaved $MAPbBr_3$ single crystal under O_2 exposures. From Ref. [46] with permission.

By comparing the metallic Pb ratios from the three atmospheres, it can be found that no matter when the degradations started and how long the exposures were, the ratio of the metallic Pb always saturated at 10%. This may be because that the perovskite surface was covered by the 10% metallic Pb layer which prevented it from further decomposition. It has been reported that $MAPbBr_3$ single crystal has better stability and can be stored in air for eight months [51][52][53]. In addition, oxygen exposure could enhance photoluminescence (PL) performance of the $MAPbBr_3$ single crystal [54].

3.4. $MAPbBr_3$ Single Crystal Stability with Water Exposure

Similar to the perovskite thin film, perovskite SC may also vulnerable to moisture. Figure 9 shows the evolution of five major elements and the VB region. The whole exposure process can also be divided into two stages.

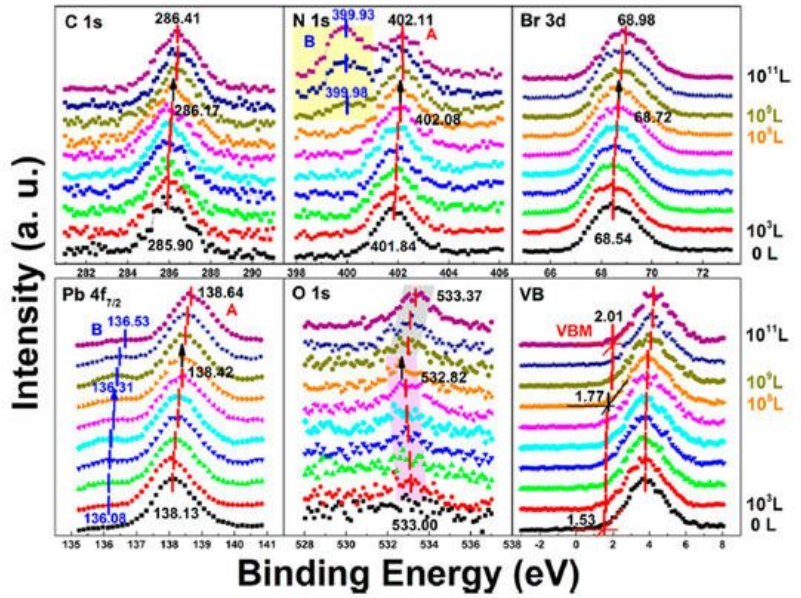

Figure 9. Evolution of C 1s, N 1s, Br 3d, Pb $4f_{7/2}$, O 1s, and the VB region of cleaved $MAPbBr_3$ single crystal under water exposure from 0 to 10^{11} L. From Ref. [46] with permission.

In stage one, the metallic Pb peak appeared at ~136.08 eV from the second scan which was caused by X-ray degradation. There is no obvious signal for oxygen from the freshly cleaved sample and the oxygen peak started to show up at ~533.00 eV from 10^3 L, which can be attributed to water. Then it moved toward the lower BE direction with a maximum of ~0.18 eV at 10^8 L. This displacement in opposite direction indicates that there was no chemical reaction between water and the SC during this stage.

The ratio is C/N/Pb/Br/O = 1.53:1.10:1:2.92: for the freshly cleaved $MAPbBr_3$ SC. Similar with X-ray degradation, the following mechanism is proposed for step one in water exposure [47].

$$CH_3NH_3Br \overset{H2O+Xray}{\rightarrow} CH_3NH_2(g) + HBr\uparrow$$

There is ~30% MABr from the diffusion and the X-ray degradation further decomposed into CH_3NH_2 and HBr gases under X-ray with 14% doped water and then escaped the sample surface.

In the second stage, $MAPbBr_3$ SC started to react with water from 10^9 L as two noticeable changes are shown in Figure 9. First, the O 1s quickly moved to the higher BE direction by ~0.55 eV, which was the same for the other major peaks but opposite from that before 10^8 L. Second, there was a second nitrogen peak (N 1s-B) showed up at ~399.98 eV, which may be caused by NH_4^+ formed by the reaction of NH_3 and H_2O. These results strongly demonstrate that water was a key factor causing decomposition of perovskite SC in the second step. After the exposure, Fermi level was moved to 0.29 eV, as the bandgap is 2.3 eV for the $MAPbBr_3$ SC, which indicates a very n-type doping.

Metallic Pb increased 17% while the saturate ratio is only 10% under the same X-ray exposure condition. The extra metallic Pb may attribute to X-ray degradation of $PbBr_2$, which is from $MAPbBr_3$ and water reaction. After 10^{10} L, carbon increased ~40%, while nitrogen and bromine decreased ~39 and 32%, respectively, exposure level. Therefore, the following reactions were proposed in stage two [47].

$$CH_3NH_3PbBr_3 \overset{H_2O}{\rightarrow} (-CH_2-) + PbBr_2 + NH_3\uparrow + HBr\uparrow$$

$$PbBr_2 \overset{Xray}{\rightarrow} Pb + Br_2\uparrow$$

$$2Pb + 2H_2O + O_2 \rightarrow 2Pb(OH)_2\downarrow$$

This degradation mechanism is very similar to water degradation of the $MAPbI_3$ thin films. About 35% perovskite was decomposed into HBr and NH_3 gases by water in UHV. Partial ammonia was absorbed by water, while $PbBr_2$ was further decomposed into metallic Pb and Br_2. From 10^{10} L, white precipitate $Pb(OH)_2$ was formed by the reaction of metallic Pb, water and the residual oxygen in the chamber. Bulk crystal could be intact with some water molecules and reversible photoelectrical properties [54].

3.5. $MAPbBr_3$ Single Crystal Stability with Light Exposure

The stability of $MAPbBr_3$ SC under light illumination was investigated with a blue laser, which has a wavelength of 408 nm and intensity is ~7 times the AM 1.5 irradiation. The exposed spot received a total light exposure time of 44 h. Strong chemical decomposition was observed with XPS after the light exposure. It has been reported that structural changes in the perovskite lattice were observed under illumination, which is related to the light-induced ion migration and associated defect passivation [56]. Anaya *et al*. reported that by combining in situ PL and XPS analysis, they found the formation of a negatively charged layer of adsorbed anionic oxygen species on the surface which could drive halide anions away from the illuminated areas toward the bulk of the material [57].

A new metallic Pb spectral component started to show up in the Pb core level spectra as shown in Figure 10. A new metallic Pb feature started to appear for each Pb core level after light exposure. C, N, and Br peaks also had a similar initial BE movement as shown in Figure 11. This rigid shift is corresponding to the Fermi level movement within the bandgap, which suggests the perovskite was p-doped.

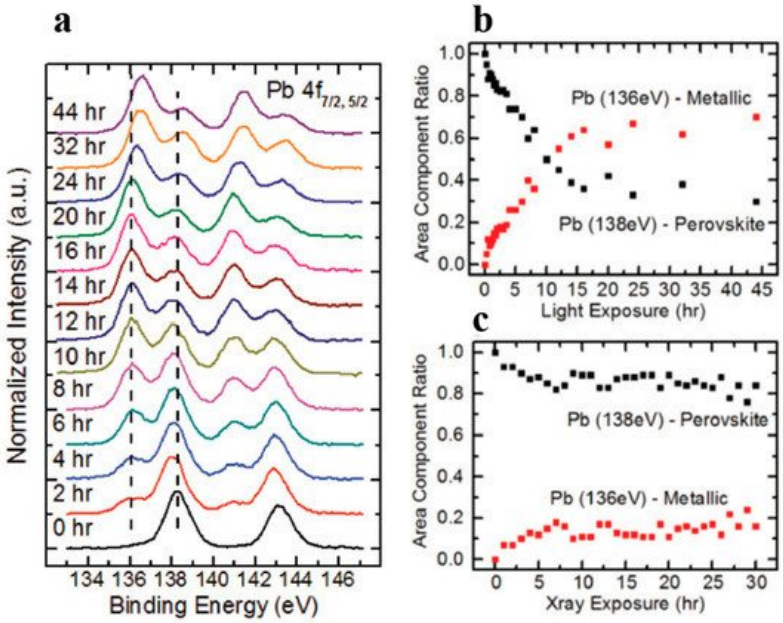

Figure 10. (**a**) A stack plot of the Pb $4f_{7/2}$ and $4f_{5/2}$ core levels of cleaved $MAPbBr_3$ single crystal with increasing light exposure. (**b**,**c**) The ratio of perovskite Pb to metallic Pb under light exposure and X-ray exposure, respectively. From Ref. [16] with permission.

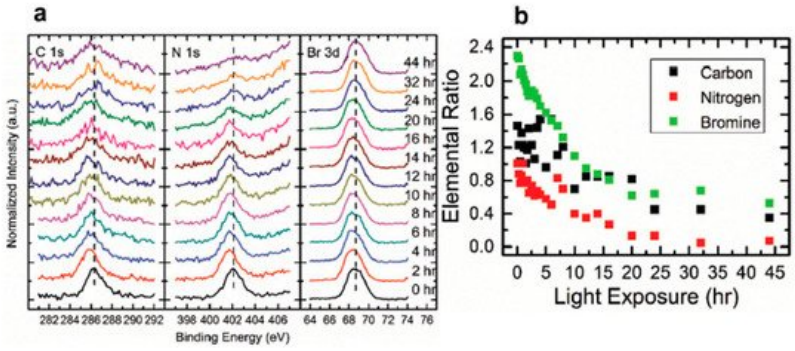

Figure 11. (**a**) A stack plot of the C 1s, N 1s, Br $3d_{5/2}$ core levels of cleaved $MAPbBr_3$ single crystal with increasing light exposure. (**b**) Elemental ratio change for C, N, and Br under light exposure. From Ref. [16] with permission.

As the light exposure progressed, the metallic Pb component continued to gain in intensity and finally dominated the overall Pb core level after ~10 h of exposure. When the whole 44 h exposure was finished, ~70% of Pb signal came from the metallic Pb, while only ~30% signal was the perovskite Pb.

For all other elements, there were no new features observed during the exposure, which suggests that they did not change their chemical states. However, the surface saw noticeable concentration losses in C, N, and Br. In Figure 11, at ~10 h of light exposure, C, N, and Br lost about half of their initial concentration, and ~50% of the perovskite Pb was degraded into metallic Pb. Based on these observations, the following mechanism was proposed to explain the degradation process [58].

$$CH_3NH_3PbBr_3 \overset{Light}{\rightarrow} CH_3NH_3Br + PbBr_2$$

$$PbBr_2 \overset{Light}{\rightarrow} Pb + Br_2$$

The perovskite SC first degraded into MABr and $PbBr_2$, then $PbBr_2$ further degrade into metallic Pb and Br_2 under light exposure. C, N, and Br were decomposed as volatile species, then escape the sample surface similar to simple outgassing. Interestingly, a similar degradation process was also observed under E-Beam Irradiation [59].

References

1. Niu, G.; Li, W.; Meng, F.; Wang, L.; Dong, H.; Qiu, Y. Study on the stability of CH 3 NH 3 PbI 3 films and the effect of post-modification by aluminum oxide in all-solid-state hybrid solar cells. J. Mater. Chem. A 2014, 2, 705–710.
2. Aristidou, N.; Sanchez-Molina, I.; Chotchuangchutchaval, T.; Brown, M.; Martinez, L.; Rath, T.; Haque, S.A. The role of oxygen in the degradation of methylammonium lead trihalide perovskite photoactive layers. Angew. Chem. 2015, 127, 8326–8330.
3. Philippe, B.; Park, B.-W.; Lindblad, R.; Oscarsson, J.; Ahmadi, S.; Johansson, E.M.; Rensmo, H.K. Chemical and Electronic Structure Characterization of Lead Halide Perovskites and Stability Behavior under Different Exposures—A Photoelectron Spectroscopy Investigation. Chem. Mater. 2015, 27, 1720–1731.
4. Lee, S.-W.; Kim, S.; Bae, S.; Cho, K.; Chung, T.; Mundt, L.E.; Lee, S.; Park, S.; Park, H.; Schubert, M.C. UV degradation and recovery of perovskite solar cells. Sci. Rep. 2016, 6, 1–10.
5. Nie, W.; Blancon, J.-C.; Neukirch, A.J.; Appavoo, K.; Tsai, H.; Chhowalla, M.; Alam, M.A.; Sfeir, M.Y.; Katan, C.; Even, J.; et al. Light-activated photocurrent degradation and self-healing in perovskite solar cells. Nat. Commun. 2016, 7, 1–9.
6. Eperon, G.E.; Stranks, S.D.; Menelaou, C.; Johnston, M.B.; Herz, L.M.; Snaith, H.J.; Science, E. Formamidinium lead trihalide: A broadly tunable perovskite for efficient planar heterojunction solar cells. Energy Environ. Sci. 2014, 7, 982–988.
7. Lee, J.W.; Kim, D.H.; Kim, H.S.; Seo, S.W.; Cho, S.M.; Park, N.-G. Formamidinium and cesium hybridization for photo- and moisture-stable perovskite solar cell. Adv. Energy Mater. 2015, 5, 1501310.
8. Wang, S.; Jiang, Y.; Juarez-Perez, E.J.; Ono, L.K.; Qi, Y.B. Accelerated degradation of methylammonium lead iodide perovskites induced by exposure to iodine vapour. Nat. Energy 2017, 2, 16195.
9. Xiao, Z.; Yuan, Y.; Shao, Y.; Wang, Q.; Dong, Q.; Bi, C.; Sharma, P.; Gruverman, A.; Huang, J. Giant switchable photovoltaic effect in organometal trihalide perovskite devices. Nat. Mater. 2015, 14, 193–198.
10. Boyd, C.C.; Cheacharoen, R.; Leijtens, T.; McGehee, M.D. Understanding degradation mechanisms and improving stability of perovskite photovoltaics. Chem. Rev. 2018, 119, 3418–3451.
11. Rolston, N.; Printz, A.D.; Tracy, J.M.; Weerasinghe, H.C.; Vak, D.; Haur, L.J.; Priyadarshi, A.; Mathews, N.; Slotcavage, D.J.; McGehee, M.D. Effect of cation composition on the mechanical stability of perovskite solar cells. Adv. Energy Mater. 2018, 8, 1702116.
12. Leijtens, T.; Eperon, G.E.; Pathak, S.; Abate, A.; Lee, M.M.; Snaith, H.J. Overcoming ultraviolet light instability of sensitized TiO2 with meso-superstructured organometal tri-halide perovskite solar cells. Nat. Commun. 2013, 4, 1–8.
13. Wang, C.; Li, Y.; Xu, X.; Wang, C.; Xie, F.; Gao, Y. Degradation of co-evaporated perovskite thin film in air. Chem. Phys. Lett. 2016, 649, 151–155.
14. Ralaiarisoa, M.; Salzmann, I.; Zu, F.-S.; Koch, N. Effect of water, oxygen, and air exposure on CH3NH3PbI3–xClx perovskite surface electronic properties. Adv. Electron. Mater. 2018, 4, 1800307.
15. Cao, K.; Zuo, Z.; Cui, J.; Shen, Y.; Moehl, T.; Zakeeruddin, S.M.; Grätzel, M.; Wang, M. Efficient screen printed perovskite solar cells based on mesoscopic TiO2/Al2O3/NiO/carbon architecture. Nano Energy 2015, 17, 171–179.
16. Eperon, G.E.; Habisreutinger, S.N.; Leijtens, T.; Bruijnaers, B.J.; van Franeker, J.J.; DeQuilettes, D.W.; Pathak, S.; Sutton, R.J.; Grancini, G.; Ginger, D.S.; et al. The importance of moisture in hybrid lead halide perovskite thin film fabrication. ACS Nano 2015, 9, 9380–9393.
17. You, J.; Yang, Y.; Hong, Z.; Song, T.-B.; Meng, L.; Liu, Y.; Jiang, C.; Zhou, H.; Chang, W.-H.; Li, G.; et al. Moisture assisted perovskite film growth for high performance solar cells. Appl. Phys. Lett. 2014, 105, 183902.
18. Dubey, A.; Kantack, N.; Adhikari, N.; Reza, K.M.; Venkatesan, S.; Kumar, M.; Khatiwada, D.; Darling, S.; Qiao, Q. Room temperature, air crystallized perovskite film for high performance solar cells. J. Mater. Chem. A 2016, 4, 10231–10240.
19. Shirayama, M.; Kato, M.; Miyadera, T.; Sugita, T.; Fujiseki, T.; Hara, S.; Kadowaki, H.; Murata, D.; Chikamatsu, M.; Fujiwara, H. Degradation mechanism of CH3NH3PbI3 perovskite materials upon exposure to humid air. J. Appl. Phys. 2016, 119, 115501.
20. Yang, J.; Siempelkamp, B.D.; Liu, D.; Kelly, T.D. Investigation of CH3NH3PbI3 degradation rates and mechanisms in controlled humidity environments using in situ techniques. ACS Nano 2015, 9, 1955–1963.
21. Sun, Q.; Fassl, P.; Becker-Koch, D.; Bausch, A.; Rivkin, B.; Bai, S.; Hopkinson, P.E.; Snaith, H.J.; Vaynzof, Y. Role of microstructure in oxygen induced photodegradation of methylammonium lead triiodide perovskite films. Adv. Energy

Mater. 2017, 7, 1700977.

22. Li, Y.; Xu, X.; Wang, C.; Wang, C.; Xie, F.; Yang, J.; Gao, Y. Degradation by Exposure of Coevaporated CH3NH3PbI3 Thin Films. J. Phys. Chem. C 2015, 119, 23996–24002.
23. Aristidou, N.; Eames, C.; Sanchez-Molina, I.; Bu, X.; Kosco, J.; Islam, M.S.; Haque, S.A. Fast oxygen diffusion and iodide defects mediate oxygen-induced degradation of perovskite solar cells. Nat. Commun. 2017, 8, 15218.
24. Kim, J.; Schelhas, L.T.; Stone, K.H. Effects of Oxygen and Water on the Formation and Degradation Processes of (CH3NH3) PbI3 Thin Films. ACS Appl. Energy Mater. 2020, 3, 11269–11274.
25. Ma, Y.; Zheng, L.; Chung, Y.-H.; Chu, S.; Xiao, L.; Chen, Z.; Wang, S.; Qu, B.; Gong, Q.; Wu, Z.; et al. A highly efficient mesoscopic solar cell based on CH 3 NH 3 PbI 3− x Cl x fabricated via sequential solution deposition. Chem. Commun. 2014, 50, 12458–12461.
26. Conings, B.; Baeten, L.; De Dobbelaere, C.; D'Haen, J.; Manca, J.; Boyen, H.G. Perovskite-based hybrid solar cells exceeding 10% efficiency with high reproducibility using a thin film sandwich approach. Adv. Mater. 2014, 26, 2041–2046.
27. Zu, F.S.; Amsalem, P.; Salzmann, I.; Wang, R.B.; Ralaiarisoa, M.; Kowarik, S.; Duhm, S.; Koch, N. Impact of white light illumination on the electronic and chemical structures of mixed halide and single crystal perovskites. Adv. Opt. Mater. 2017, 5, 1700139.
28. Christians, J.A.; Miranda Herrera, P.A.; Kamat, P.V. Transformation of the excited state and photovoltaic efficiency of CH3NH3PbI3 perovskite upon controlled exposure to humidified air. J. Am. Chem. Soc. 2015, 137, 1530–1538.
29. Leguy, A.M.; Hu, Y.; Campoy-Quiles, M.; Alonso, M.I.; Weber, O.J.; Azarhoosh, P.; Van Schilfgaarde, M.; Weller, M.T.; Bein, T.; Nelson, J.; et al. Reversible hydration of CH3NH3PbI3 in films, single crystals, and solar cells. Chem. Mater. 2015, 27, 3397–3407.
30. Nist X-Ray Photoelectron Spectroscopy Database. Available online: (accessed on 17 December 2020).
31. Ke, J.C.-R.; Walton, A.S.; Lewis, D.J.; Tedstone, A.; O'Brien, P.; Thomas, A.G.; Flavell, W.R. In situ investigation of degradation at organometal halide perovskite surfaces by X-ray photoelectron spectroscopy at realistic water vapour pressure. Chem. Commun. 2017, 53, 5231–5234.
32. Weast, R.C.; Astle, M.J.; Beyer, W.H. (Eds.) CRC Handbook of Chemistry and Physics; CRC Press: Boca Raton, FL, USA, 1985.
33. Murugadoss, G.; Tanaka, S.; Mizuta, G.; Kanaya, S.; Nishino, H.; Umeyama, T.; Imahori, H.; Ito, S. Light stability tests of methylammonium and formamidinium Pb-halide perovskites for solar cell applications. Jpn. J. Appl. Phys. 2015, 54, 08KF08.
34. Bryant, D.; Aristidou, N.; Pont, S.; Sanchez-Molina, I.; Chotchunangatchaval, T.; Wheeler, S.; Durrant, J.R.; Haque, S.A. Light and oxygen induced degradation limits the operational stability of methylammonium lead triiodide perovskite solar cells. Energy Environ. Sci. 2016, 9, 1655–1660.
35. Das, C.; Wussler, M.; Hellmann, T.; Mayer, T.; Jaegermann, W. In situ XPS study of the surface chemistry of MAPI solar cells under operating conditions in vacuum. Phys. Chem. Chem. Phys. 2018, 20, 17180–17187.
36. Zhao, J.; Deng, Y.; Wei, H.; Zheng, X.; Yu, Z.; Shao, Y.; Shield, J.E.; Huang, J. Strained hybrid perovskite thin films and their impact on the intrinsic stability of perovskite solar cells. Sci. Adv. 2017, 3, eaao5616.
37. Yuan, H.; Debroye, E.; Janssen, K.; Naiki, H.; Steuwe, C.; Lu, G.; Moris, M.I.; Orgiu, E.; Uji-i, H.; De Schryver, F.; et al. Degradation of methylammonium lead iodide perovskite structures through light and electron beam driven ion migration. J. Phys. Chem. Lett. 2016, 7, 561–566.
38. Li, Y.Z.; Xu, X.R.; Wang, C.C.; Ecker, B.; Yang, J.L.; Huang, J.; Gao, Y.L. Light-Induced Degradation of CH3NH3PbI3 Hybrid Perovskite Thin Film. J. Phys. Chem. C 2017, 121, 3904–3910.
39. Sadoughi, G.; Starr, D.E.; Handick, E.; Stranks, S.D.; Gorgoi, M.; Wilks, R.G.; Bär, M.; Snaith, H.J. Observation and mediation of the presence of metallic lead in organic-inorganic perovskite films. ACS Appl. Mater. Interfaces 2015, 7, 13440–13444.
40. Liu, L.; McLeod, J.A.; Wang, R.; Shen, P.; Duhm, S. Tracking the formation of methylammonium lead triiodide perovskite. Appl. Phys. Lett. 2015, 107, 061904.
41. Wang, Q.; Shao, Y.; Xie, H.; Lyu, L.; Liu, X.; Gao, Y.; Huang, J. Qualifying composition dependent p and n self-doping in CH3NH3PbI3. Appl. Phys. Lett. 2014, 105, 163508.
42. Park, R.L.; Lagally, M.G. Solid State Physics: Surfaces; Academic Press: Cambridge, MA, USA, 1985; Volume 22.
43. Huang, W.; Manser, J.S.; Kamat, P.V.; Ptasinska, S. Evolution of chemical composition, morphology, and photovoltaic efficiency of CH3NH3PbI3 perovskite under ambient conditions. Chem. Mater. 2016, 28, 303–311.

44. Tang, X.; Brandl, M.; May, B.; Levchuk, I.; Hou, Y.; Richter, M.; Chen, H.; Chen, S.; Kahmann, S.; Osvet, A.; et al. Photoinduced degradation of methylammonium lead triiodide perovskite semiconductors. J. Mater. Chem. A 2016, 4, 15896–15903.
45. Domanski, K.; Roose, B.; Matsui, T.; Saliba, M.; Turren-Cruz, S.-H.; Correa-Baena, J.-P.; Carmona, C.R.; Richardson, G.; Foster, J.M.; De Angelis, F.; et al. Migration of cations induces reversible performance losses over day/night cycling in perovskite solar cells. Energy Environ. Sci. 2017, 10, 604–613.
46. Kazim, S.; Nazeeruddin, M.K.; Grätzel, M.; Ahmad, S. Perovskite as light harvester: A game changer in photovoltaics. Angew. Chem. Int. Ed. 2014, 53, 2812–2824.
47. Wang, C.; Ecker, B.R.; Wei, H.; Huang, J.; Gao, Y. Environmental Surface Stability of the MAPbBr3 Single Crystal. J. Phys. Chem. C 2018, 122, 3513–3522.
48. Dong, X.; Fang, X.; Lv, M.; Lin, B.; Zhang, S.; Ding, J.; Yuan, N. Improvement of the humidity stability of organic-inorganic perovskite solar cells using ultrathin Al2O3 layers prepared by atomic layer deposition. J. Mater. Chem. A 2015, 3, 5360–5367.
49. Wang, Y.-K.; Yuan, Z.-C.; Shi, G.-Z.; Li, Y.-X.; Li, Q.; Hui, F.; Sun, B.-Q.; Jiang, Z.-Q.; Liao, L.-S. Dopant-free spiro-triphenylamine/fluorene as hole-transporting material for perovskite solar cells with enhanced efficiency and stability. Adv. Funct. Mater. 2016, 26, 1375–1381.
50. Zhu, Z.; Hadjiev, V.G.; Rong, Y.; Guo, R.; Cao, B.; Tang, Z.; Qin, F.; Li, Y.; Wang, Y.; Hao, F.; et al. Interaction of organic cation with water molecule in perovskite MAPbI3: From dynamic orientational disorder to hydrogen bonding. Chem. Mater. 2016, 28, 7385–7393.
51. Zhou, Y.; Li, C.; Wang, Y.; Du, X.; Liu, P.; Xie, W. Preparation and characterization of high-quality perovskite CH3NH3PbX3 (I, Br) single crystal. In IOP Conference Series: Materials Science and Engineering; IOP Publishing: Bristol, UK, 2017.
52. Liu, Y.; Yang, Z.; Cui, D.; Ren, X.; Sun, J.; Liu, X.; Zhang, J.; Wei, Q.; Fan, H.; Yu, F.; et al. Two-inch-sized perovskite CH3NH3PbX3 (X = Cl, Br, I) crystals: Growth and characterization. Adv. Mater. 2015, 27, 5176–5183.
53. Liu, Y.; Zhang, Y.; Zhao, K.; Yang, Z.; Feng, J.; Zhang, X.; Wang, K.; Meng, L.; Ye, H.; Liu, M.; et al. A 1300 mm2 ultrahigh-performance digital imaging assembly using high-quality perovskite single crystals. Adv. Mater. 2018, 30, 1707314.
54. Fang, H.-H.; Adjokatse, S.; Wei, H.; Yang, J.; Blake, G.R.; Huang, J. Ultrahigh sensitivity of methylammonium lead tribromide perovskite single crystals to environmental gases. Sci. Adv. 2016, 2, e1600534.
55. Murali, B.; Dey, S.; Abdelhady, A.L.; Peng, W.; Alarousu, E.; Kirmani, A.R.; Cho, N.; Sarmah, S.P.; Parida, M.R.; Saidaminov, M.I.; et al. Surface restructuring of hybrid perovskite crystals. ACS Energy Lett. 2016, 1, 1119–1126.
56. Galisteo-López, J.F.; Calvo, M.E.; Míguez, H. Spatially Resolved Analysis of Defect Annihilation and Recovery Dynamics in Metal Halide Perovskite Single Crystals. ACS Appl. Energy Mater. 2019, 2, 6967–6972.
57. Anaya, M.; Galisteo-López, J.F.; Calvo, M.E.; Espinós, J.P.; Míguez, H. Origin of light-induced photophysical effects in organic metal halide perovskites in the presence of oxygen. J. Phys. Chem. Lett. 2018, 9, 3891–3896.
58. Ecker, B.R.; Wang, C.; Wei, H.; Yuan, Y.; Huang, J.; Gao, Y. Intrinsic Behavior of CH3NH3PbBr3 Single Crystals under Light Illumination. Adv. Mater. Interfaces 2018, 5, 1801206.
59. Syafutra, H.; Yun, J.-H.; Yoshie, Y.; Lyu, M.; Takeda, S.N.; Nakamura, M.; Wang, L.; Jung, M.-C. Surface Degradation Mechanism on CH3NH3PbBr3 Hybrid Perovskite Single Crystal by a Grazing E-Beam Irradiation. Nanomaterials 2020, 10, 1253.